International Journal of Cardiology 220 (2016) 32–42

Contents lists available at ScienceDirect

International Journal of Cardiology

journal homepage: www.elsevier.com/locate/ijcard

Prevalence of parameters of suboptimal scaffold deployment following angiographic guided bioresorbable vascular scaffold implantation in real world practice - an optical coherence tomography analysis

Vijayakumar Subban [a,*,1], Gunasekaran Sengottuvelu [b,1], Kalaichelvan Uthayakumaran [a,1], Ravindran Rajendran [b,1], Ezhilan Janakiraman [a,1], Balaji Pakshirajan [a,1], Jose G. Thenpally [a,1], Latchumanadhas Kalidoss [a,1], Suma M. Victor [a,1], Mathew Samuel Kalarickal [b,1], Mullasari S. Ajit [a,1]

[a] Institute of Cardiovascular Diseases, The Madras Medical Mission, Chennai, India
[b] Department of Cardiology, Apollo Hospitals, Chennai, India

ARTICLE INFO

Article history:
Received 11 January 2016
Received in revised form 19 May 2016
Accepted 21 June 2016
Available online 23 June 2016

Keywords:
Optical coherence tomography
Bioresorbable vascular scaffold
Suboptimal implantation

ABSTRACT

Aim: To assess the prevalence of suboptimal bioresorbable vascular scaffold (BVS, Abbott Vascular, Santa Clara, California) deployment in real world practice with intracoronary optical coherence tomography (OCT) imaging.
Methods: Consecutive patients who underwent percutaneous coronary intervention using BVS and the final optimization assessed with OCT imaging in two tertiary care centers between December 2012 and February 2015 were evaluated for parameters of suboptimal scaffold deployment by OCT.
Results: Overall, 36 scaffolds were implanted in 27 patients during this period. Mean age of the population was 54.7 ± 8.2 years and 19 (70.4%) were type B2/C lesions. The prevalence of parameters of suboptimal scaffold deployment were: underexpansion-22(61.1%), geographic miss-3(8.3%), tissue prolapse-7(25.9%), scaffold pattern irregularity-1(2.8%), longitudinal elongation-7(38.8%). Of the 7 overlaps imaged: excessive overlap was observed in 3 and scaffold gap in one. The median duration of follow up was 679 days (range 193–963 days). There were four events during this period. None were associated with suboptimal scaffold deployment.
Conclusion: OCT based parameters of suboptimal scaffold deployment are common in real world scenario and were not associated with adverse outcomes on long term follow up. These findings need to be confirmed in larger studies.

1. Introduction

Bioresorbable vascular scaffold (BVS, Absorb, Abbott Vascular, Santa Clara, California) is a new generation device and considered as the fourth revolution in the evaluation of coronary stent technology. BVS is made up of bioresorbable polymer (poly-L-lactic acid) backbone and coated with bioresorbable polymer (poly-DL-lactic acid) and anti-proliferative drug, everolimus. The scaffold is completely resorbed over a period of 24–48 months and leaves the vessel free of permanent metallic caging. This offers a number of advantages over the current generation drug eluting stents (DES) and may potentially alleviate most of the long term problems associated with them. Similar to DES, the scaffold provides mechanical support to counteract the acute vessel recoil post angioplasty and the drug elution limits excessive neointimal growth. In contrast, its flexibility and conformability preserves the vessel geometry and bioresorption restores vasomotion, prevents permanent jailing of the side branch ostium, and frees the segment for late bypass grafting and also results in late luminal gain and expansive remodeling. In addition, it may eliminate the risk of very late stent thrombosis and the need for long term dual anti-platelet therapy [1]. With promising outcomes from the first in man study [2] and subsequent registries [3,4], BVS is currently being implanted in more complex clinical subsets and the acute performance and the clinical outcomes have been shown to be comparable to that of DES [5,6].

Though BVS promises numerous improvements over DES, it may not be totally immune to the acute and late failures (stent thrombosis and restenosis) associated with DES. With increasing usage of BVS in the real world scenarios and complex lesion subsets, the scaffold failures are increasingly being recognized [7]. Importantly, the main mode of failure was scaffold thrombosis and the most of the events clustered

* Corresponding author at: Institute of Cardiovascular Diseases, The Madras Medical Mission, 4A, Dr. JJ Nagar, Mogappair, Chennai 600037, India.
E-mail address: drkumarvijay@gmail.com (V. Subban).
[1] This author takes responsibility for all aspects of the reliability and freedom from bias of the data presented and their discussed interpretation.

http://dx.doi.org/10.1016/j.ijcard.2016.06.096
0167-5273/

to the early period following scaffold implantation. This implicates suboptimal scaffold implantation as the possible pathological mechanism of scaffold thrombosis [7]. In addition, intravascular imaging studies have shown the same pathologic mechanisms of DES failure, such as underexpansion, gross malapposition and geographic miss in patients presenting with scaffold thrombosis [8,9]. Similarly, there was evidence of suboptimal scaffold implantation in patients with scaffold restenosis [10,11]. Further, unlike metallic stents, the scaffold is prone to deformation with overexpansion [12] and longitudinal elongation [13] with high pressure dilatation in the presence of resistant plaques. Importantly, poor angiographic visibility of BVS, makes it difficult to recognize these abnormalities with angiography alone.

The current study retrospectively analyzed in detail the prevalence of such markers of suboptimal scaffold deployment with optimal coherence tomography (OCT) and correlates them with clinical outcomes during follow up.

2. Methods

The study population included consecutive patients who underwent percutaneous coronary intervention (PCI) using BVS and the final optimization assessed with OCT imaging in two tertiary care centers (the Madras Medical Mission, and the Apollo hospital) in Chennai, India between December 2012 and February 2015. There were no specific exclusion criteria except for the angiographic vessel size assessed visually by the operator not suitable for the currently available scaffold sizes.

All the scaffolds were implanted by 4 experienced operators. Aggressive lesion preparation was recommended and the strategy was left to operator's preference. There was no routine preprocedural QCA or OCT assessment. Scaffold selection was based on visual assessment of vessel size by the operator. All the scaffolds were implanted as per manufacturer's recommendation. Routine post dilatation was recommended with noncompliant balloon sized to the scaffold or within the expansion range of the particular scaffold. When overlapping of scaffolds was required, marker-to-marker or scaffold-to-scaffold technique was used. In case of bifurcation lesions, either provisional technique with or without snuggle balloon dilation or two scaffold T technique with final kissing balloon dilatation was used. Once optimal scaffold deployment was confirmed angiographically, OCT imaging was obtained. Further scaffold optimization based on the OCT findings were allowed and a final OCT imaging was acquired in the end. All the OCT imaging were performed with either Ilumien™ or Ilumien™ Optis™ PCI optimization system (St. Jude Medical, Minneapolis, Minnesota) using DragonFly™ imaging catheter (St. Jude Medical) at a pullback speed of either 10 mm or 20 mm per second with manual contrast flushing. Imaging was repeated when the pullback was not optimal and additional imaging was performed when the pullback was not enough to cover the full length of the scaffold.

Baseline demographic and clinical data and the procedural details such as type of the pre-dilatation/post-dilatation balloons used, the maximal diameter and maximal inflation pressure were collected from the case records.

All the angiographic and OCT data were collected retrospectively and analyzed by two independent observers at a core laboratory (Indian Cardiology Research Foundation, Chennai, India). The angiographic analysis was performed with CASS 5.10.2 software (Pie Medical BV, Maastricht, Netherlands). Lesions were categorized into different types based on ACC/AHA task force criteria for coronary lesion classification [14]. The minimal lumen diameter (MLD, smallest diameter in the lesion segment), angiographic percentage diameter stenosis (DS, [reference lumen diameter − minimal lumen diameter/reference lumen diameter] × 100), the interpolated reference vessel diameter (RVD, predicted reference diameter at the site of MLD), maximal vessel diameter (Dmax, largest reference diameters proximal and distal to the lesion) and the length of the obstruction were obtained in the preprocedural angiogram [15]. Post procedure QCA analysis included the lesion as a whole rather than individual scaffolds in patients with overlapping scaffolds. The treated segment and the peri-scaffold areas (5 mm both proximal and distal to the scaffold) were analyzed in the final angiogram and MLD, DS and acute lumen gain were obtained. Epicardial flow in the target artery was categorized as per TIMI flow grading criteria [14].

OCT analysis was performed offline using a dedicated OCT work station (Ilumien™ Optis™, St. Jude Medical) as per previous recommendations [16]. Cross sections were analyzed at 1 mm intervals in the scaffold segment and 5 mm proximal and distal to the scaffold. The frames where $>90^0$ of the circumference was not suitable for analysis, were excluded. The scaffold struts are translucent and appear as black boxes with high back-scattering borders that allow the assessment of the vessel wall behind the struts. In each frame, observation was made for presence of malapposition (lack of contact between scaffold and vessel wall), tissue prolapse (plaque or thrombus protruding between the struts) and scaffold pattern irregularity/fracture (SPI/F, presence of a 2nd strut overhanging in the same angular sector or a free floating strut close to the center of the lumen). The total number struts and those with malapposition in each scaffold were counted and the percentage of malapposed struts per scaffold was then calculated. In each frame, the lumen area, scaffold area, maximal and minimal diameter were obtained. The lumen area was traced at the tissue border behind the scaffold in the absence of tissue prolapse and is equal to the scaffold area in the absence of malapposition and larger than the scaffold area in the presence of malapposition. In the areas of tissue prolapse, the lumen area was traced along the tissue inside the scaffold. Tissue prolapse area was derived from subtracting the lumen area from the scaffold area. Optimal scaffold expansion was defined as scaffold minimal cross sectional area (CSA) of more than 80% of the maximum expected area for the scaffold used. For 2.5 mm, 3 mm and 3.5 mm scaffolds the optimal areas were 4 mm^2, 6 mm^2 and 8 mm^2 respectively [17]. Scaffolds not meeting these criteria were defined as underexpanded. Malapposition was classified into following types: under-deployment related (malapposition resulting from correctly sized scaffold deployed at low pressure), under-sized scaffold related (malapposition resulting from undersized scaffold), plaque related (fibro-calcific plaque preventing strut apposing to the vessel wall), ectasia related (malapposition resulting from large lumen dimensions at the ectatic segment), overhang/protrusion related (malapposition resulting from scaffold overhang in to the proximal main vessel), side branch related (malapposition at the site of side branches), scaffold fracture related (malapposition related to scaffold fracture – malapposed overhanging or free strut). Side branch related malapposition was excluded from the analysis. Presence of >5% of the struts with malapposition in a scaffold was considered significant. Tissue prolapse occupying >10% of the scaffold area was considered abnormal. The proximal and distal edges were assessed for the presence of dissection (breach in the endoluminal continuity), intramural hematoma (accumulation of blood in the medial space) and geographic miss (Inadequate lumen area - <4 mm^2/large uncovered plaque or dilated segment at the scaffold edges). Edge dissection was defined as major when it occupies >60% of the lumen circumference and the residual lumen area < 4 mm^2 [18]. In case of overlapping scaffolds, presence of excessive overlap (stacking of struts of adjacent scaffolds for >1 mm length) or scaffold gap (gap between the scaffolds at the overlapping site) was noted. For scaffolds implanted in the ostial position, the length of overhang was measured. Overhang of >1 mm was considered excessive. The scaffolds where there was no overlap and both proximal and distal edges clearly visible were assessed for elongation (measured length longer than the predicted length). The scaffold edge was defined as the first frame with <3 quadrants of scaffold identified in a cross section at either ends. The calibration was adjusted before each measurement [13]. All the length measurements were done thrice by each examiner and the average value was taken. In addition, symmetry

index (ratio of the difference between maximum and minimum diameters to the maximum diameter in a scaffold) and eccentricity index per frame (Ratio of minimum scaffold diameter to the maximum scaffold diameter in the same frame) and mean eccentricity index per scaffold were calculated [16].

The scaffolds with one or more of the following were considered suboptimally deployed: underexpansion, malapposition of >5% struts, geographic miss, major dissection/hematoma, significant tissue prolapse, excessive overhang, elongation, scaffold pattern abnormalities.

All patients received dual antiplatelet therapy. Patients with any of the above abnormalities were put on either prasugrel or ticagrelor and were advised to continue it for a duration of 4 years unless the bleeding risk was high.

Patients were followed up clinically at 1 month, 6 months, 12 months and yearly thereafter up to 4 years. Data before January 2015 were collected from the follow up case records and were prospectively followed after this period. An angiogram and an OCT imaging was obtained if the patient presented with clinical symptoms of ischemia/stress studies suggestive of inducible ischemia during the follow up period. Otherwise a routine angiography with OCT imaging is planned at the completion of 48 month (the proposed period for complete disappearance of the scaffold).

3. Results

Overall, 36 scaffolds were implanted with OCT assessment of final optimization in 27 patients during this period. The demographic and clinical characteristics are shown in Table 1. Briefly, 20(74.1%) patients were males and the mean age of the population was 54.7 ± 8.2 years. 12 patients (44.4%) presented with acute coronary syndrome and six of them were following ST-segment elevation myocardial infarction (STEMI).

The baseline and procedural data are summarized in Table 2. Left anterior descending coronary artery (LAD) was the most common target vessel (55.6%) and 19 (70.4%) were type B2/C lesions. The final epicardial flow was TIMI III in all of them. All but two patients underwent balloon predilatation and the mean balloon to scaffold ratio was 0.9 ± 0.12. All the scaffolds were deployed successfully. 15 (45.5%) scaffolds were post dilated with upsized balloons. QCA parameters are shown in Table 3. Based on the Dmax and interpolated reference diameter criteria 29 (80.6%) and 24 (66.7%) scaffolds were appropriately sized. 12 (44.4%) lesions showed final residual stenosis of >20% by QCA.

OCT data are displayed in Table 4. 47 pull backs were performed in total. Overall, 959 frames and 6427 struts were analyzed. The mean scaffold areas for 2.5 mm, 3 mm and 3.5 mm scaffolds were 5.3 ± 1.6 mm^2, 6.44 ± 1.76 mm^2 and 10.5 ± 1.8 mm^2 respectively. Scaffold underexpansion was observed in 22 (66.1%) scaffolds and 145(15.1%) frames and was more common with 3 mm scaffolds. 5 of the 3 mm scaffolds were implanted in smaller vessels (Dmax < 2.5 mm) where 2.5 mm scaffolds would have been more appropriate. Even when, 4 mm^2 criteria was applied to these scaffolds, 4 scaffolds and 20 frames still remained under expanded (Fig. 1). None of the scaffolds showed malapposition involving >5% of the struts. Significant tissue prolapse was noted in 7 (25.9%) scaffolds and no further intervention was done in any of them. There were 6

Table 1
Demographic and clinical characteristics.

Total no of patients	27
Age in years (Sdev)	54.70 (8.18)
Male (%)	20 (74.07)
Female (%)	7 (25.92)
Diabetes mellitus (%)	12 (44.44)
Hypertension (%)	13 (48.14)
Dyslipidemia (%)	2 (7.40)
Ex-smoker (%)	1 (3.70)
Current smoker (%)	5 (18.51)
Previous PTCA (%)	1 (3.70)
Previous CABG (%)	3 (11.11)
Cerebrovascular accident (%)	2 (7.40)
Chronic kidney disease (%)	2 (7.40)
Clinical presentation	
Stable angina (%)	15 (55.6)
Unstable angina (%)	2 (7.40)
Non ST – segment elevation myocardial infarction (%)	4 (14.3)
ST – segment elevation myocardial infarction (%)	6 (22.22)

Table 2
Baseline lesion and procedural characteristics.

Target vessel	LAD/D (%)	15 (55.55)
	RCA/PDA (%)	6 (22.22)
	LCX/OM (%)	4 (14.28)
	GRAFT (%)	2 (7.40)
Lesion type	A (%)	8 (29.62)
	B2 (%)	7(25.92)
	C (%)	12 (44.44)
Calcified lesion (%)		1 (3.70)
ST – segment elevation myocardial infarction (%)		1 (3.70)
2 stent bifurcation (%)		3 (11.11)
Single stent bifurcation (%)		3 (11.11)
Long lesion (%)		4 (14.81)
Ostial stenting (%)		2 (7.4)
TIMI grade	Pre (%)	Post (%)
0	1(3.57)	0
1	1 (3.57)	0
2	5 (17.85)	0
3	21 (75)	27 (100)
Pre-dilatation (%)		25 (92.5)
Semi complaint balloon (%)		11 (40.74)
Non-complaint balloon (%)		19 (70.34)
Cutting balloon (%)		2 (7.40)
Balloon to scaffold ratio ± Sdev		0.90 ± 0.12
Maximal pre dilatation balloon inflation pressure		14 ± 3.18
Total number of Scaffolds		36
Scaffold per person (Sdev)		1.33 ± 0.62
Scaffold Length per patient - mm (Sdev)		30.67 ± 15.93
Scaffold median size -mm (Range)		3 (2.5, 3.5)
Scaffold median length -mm (Range)		18 (18, 28)
No of patients with Overlapping scaffolds (%)		6 (22.22)
Total number of overlaps		8
Scaffold deployment pressure (ATM) ± Sdev		9.32 ± 2.38
Post-dilatation (%)		33 (91.67)
Non-compliant balloon (%)		33 (91.67)
No of scaffolds dilated with same size balloons (%)		18 (54.55)
No of scaffolds dilated with upsized balloons (%)		15 (45.45)
Balloon to scaffold ratio		1.05 ± 0.07
Maximal post-dilatation pressure (ATM) ± Sdev		17.7 ± 4.24

Table 3
Pre procedural and post procedural quantitative coronary analysis.

Pre-procedure	
D max – proximal (mm)	3.02 ± 0.72
D max – distal (mm)	2.45 ± 0.47
Interpolated Reference Diameter (mm)	2.48 ± 0.43
MLD (mm)	0.91 ± 0.44
Percentage diameter stenosis (%)	62.07 ± 15.57
Length of obstruction (mm)	15.81 ± 7.48
Scaffolds sizing to Q Max - appropriate (%)/oversized (%)/undersized (%)	29 (80.56)/5 (13.89)/2 (5.56)
Scaffold sizing to interpolated reference - appropriate (%)/oversized (%)/undersized (%)	24(66.67)/12 (33.34)/0
Post-procedure	
MLD (mm)	1.94 ± 0.43
Maximum lumen diameter (mm)	3.09 ± 0.47
Acute gain (mm)	0.84 ± 0.61
Percentage Diameter Stenosis (%)	20.12 ± 11.37
No of lesions with >20% residual stenosis (%)	12 (44.44)

D max – maximum diameter, MLD – minimum luminal diameter.

Table 4
Optical coherence tomography analysis.

Number of OCT pullbacks	47
Number of frames analyzed	959
Number of struts analyzed	6427
Mean scaffold area - mm^2 (Sdev)	6.55 ± 2.28
2.5 mm scaffold	5.26 ± 1.55
3 mm scaffold	6.44 ± 1.76
3.5 mm scaffold	10.47 ± 1.75
Minimum scaffold area - mm^2 (Sdev)	4.97 ± 1.60
2.5 mm scaffold	4.21 ± 0.81
3 mm scaffold	5.06 ± 1.30
3.5 mm scaffold	7.79 ± 2.04
Number of scaffolds with MLA <5 mm^2 (%)	15 (41.66)
Scaffolds with underexpansion (%)	22 (61.11)
2.5 mm scaffold	5 (41)
3 mm scaffold	16 (88)
3.5 mm scaffold	1(16)
Number of frames with underexpansion (%)	200 (20.85)
2.5 mm scaffold (%)	25/235 = 10.64
3 mm scaffold (%)	170/636 = 26.73
3.5 mm scaffold (%)	5/88 = 5.68
Oversized scaffold related underexpansion (3 mm scaffolds)/frames	5/97
Oversized 3 mm scaffold not met 2.5 mm criteria/frames	4/20
Total number of struts malapposed	199 (3.10)
Plaque related (%)	95 (1.47)
Side branch related (%)	24 (0.37)
Ectasia related (%)	16 (0.25)
Overhang related (%)	64 (1.0)
Number of scaffolds with >5% malapposition	0
Geographic miss (%)	3 (11.11)
Edge dissection/haematoma	9 (33.33)
Major (%)	3 (11.11)
Minor (%)	6 (16.66)
Scaffold pattern irregularities (%)	1(2.77)
Tissue prolapse occupying >10% of scaffold area/frames/%	7(25.93)/47 (4.90)
Number of side branch scaffolds protruding into the proximal main vessel (%)	4 (14.81)
Ostial LAD into left main	3 (1.9,1.5,2)
PDA into RCA	1 (3.8)
Number of overlaps analyzed	7
Marker inside marker overlap (>1 mm) (%)	3
Marker over marker/side by side	3
Scaffold Gaps	1
Longitudinal elongation (%)	7(38.89)
Eccentricity index – mean (Sdev)/Min (Sdev)	0.83 ± 0.05/0.70 ± 0.09
Symmetry index	0.22 ± 0.09

non-flow limiting edge dissections and a small hematoma which were left alone. Significant scaffold overhang was observed in 4 scaffolds. Three of them from LAD into left main coronary artery (1.9 mm, 1.5 mm and 2 mm respectively) and one from posterior descending coronary artery into the distal right coronary artery (RCA, 3.8 mm, Fig. 2). 2 of these overhangs were associated with 360^0 malapposition and 180^0 in the remaining two (adherent to the vessel wall on one side). Of the 7 overlaps imaged, 3 were optimal (≤1 mm overlap), 3 showed excessive overlap and there was 1 mm gap between the scaffolds in another. The maximum overlapping length was 4.9 mm in a patient where the second scaffold was implanted in a long LAD lesion. Though the scaffold markers were positioned in a marker to marker fashion, it moved distally during deployment due to calcium at the proximal edge (Fig. 3). In the patient with the gap, the scaffold was implanted to cover an edge dissection which remained partially uncovered. However, the lumen area was adequate and there were no flaps protruding into the lumen (Fig. 4). Longitudinal elongation of the scaffold was noted in 7 (38.9%) of 18 scaffolds imaged. The maximum elongation length was 1.4 mm. This scaffold was implanted in a calcified lesion after optimal lesion preparation was confirmed by OCT and scaffold achieved adequate lumen areas (Fig. 5). Geographic miss occurred in three patients. In two patients the scaffolds edges landed in areas with large plaque and small lumen area and in another patient the scaffold missed the dilated segment proximally, however the lumen area was adequate. Scaffold pattern irregularity/fracture (SPI/F) was observed in a patient who had two 3.5 mm overlapping scaffolds implanted for a long RCA lesion extending to the ostium. Large area of malapposition was observed close to the ostium and was dilated with a 3.75 mm noncompliant balloon. Final OCT imaging showed deformation of the proximal end of the scaffold probably occurred during reengagement with guiding catheter post dilatation (Fig. 6). This was not recognized during procedure and picked up only during the core lab analysis. There were 3 additional interventions performed based on the OCT findings: two for major malapposition and one for major distal edge dissection.

The median duration of follow up was 679 days (range 193–963 days). There were four events during this period. First event was in a patient who had a 3 × 18 scaffold implanted for a calcified lesion in the proximal LAD. His post procedure OCT showed optimal scaffold areas and longitudinal elongation of the scaffold (final length 19.4 mm). Patient presented with anginal symptoms 49 days post procedure. Coronary angiogram showed patent scaffold and was treated medically. The same patient presented again 556 days post procedure with chest discomfort. Angiogram showed patent scaffold and an OCT imaging was performed which showed good neointimal covering with no significant lumen narrowing. The scaffold measured a length of 18 mm. He was treated medically. The second patient had three 2.5 mm overlapping scaffolds implanted in the radial artery graft to PDA. He underwent a follow up CT angiogram at twelve months which showed patent scaffold. At the end of twenty four months, he came with worsening angina symptoms. A coronary angiogram was done which showed occluded radial artery graft and was left on medical treatment. All three scaffolds were optimally deployed by OCT criteria in this patient. The third patient presented with angina after 665 days following scaffold implantation in another centre. His angiogram showed mild scaffold in-stent restenosis (no OCT imaging performed) and a new lesion in his right coronary artery. He underwent successful PCI to RCA with a DES.

4. Discussion

The main findings of our study are: (1) suboptimal deployment of BVS is common in real world scenario, (2) angiography poorly identified the components of suboptimal scaffold implantation, (3) underexpansion was the most common form of suboptimal scaffold deployment, and (4) suboptimal deployment was not associated with any clinical events in the scaffolded segments during follow up.

4.1. Scaffold underexpansion

Underexpansion has been repeatedly shown to be a key predictor of stent failure with both BMS and DES [19,20]. Though IVUS studies have been describing it over the past 2 decades, there are no uniform criteria for the assessment of stent expansion. It has been expressed either as an absolute number (minimum stent CSA) or % of residual stenosis compared to the reference lumen area [19–22]. In a non-left main lesion, a stent area of <5 −5–5 mm^2 predicted restenosis at follow up [19,20]. There have been few case series of scaffold failure published to date and all reported cases of underexpansion in patients with scaffold failure. However, exact criterion used to measure expansion was not mentioned in any of them [8–11]. In GHOUST-EU study, there was a high incidence of angiographic residual stenosis (>20%) in patients with follow up instent restenosis [23]. Mattesini et al. [5], compared acute performance of BVS with second generation metallic stents. The median length of the scaffold used was 28 mm and they could achieve expansion similar to that of the metal stents. However, this needed aggressive lesion preparation for BVS. This study used expansion criteria of 80% of the average reference vessel diameters and did not involve long lesions requiring overlapping scaffold implantation. The expansion criteria were not met in 39.7% of the patients in the BVS group. In the

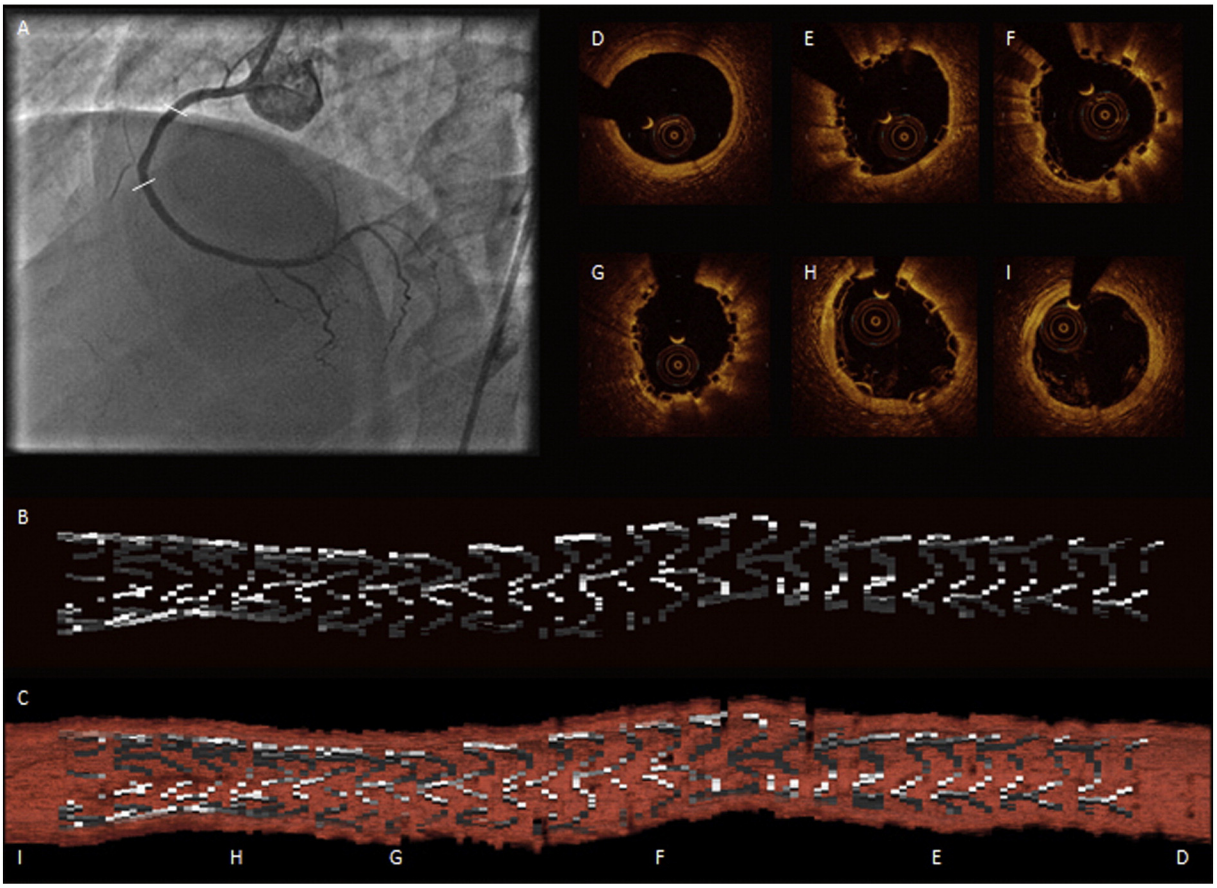

Fig. 1. Scaffold underexpansion. Patient was implanted with a 3 mm scaffold in mid RCA. (A) Angiographically optimal result. (B,C) OCT 3 D reconstruction images showing underexpanded scaffold. Crowding of struts are noted at proximal and distal thirds of the scaffold. (D–I) OCT cross sectional images showing small, disease free reference segments (D, proximal – mean diameter 2.5 mm and I, distal –mean diameter 2.4 mm) and small lumen areas (E–H). Minimum scaffold area 4.32 mm^2.

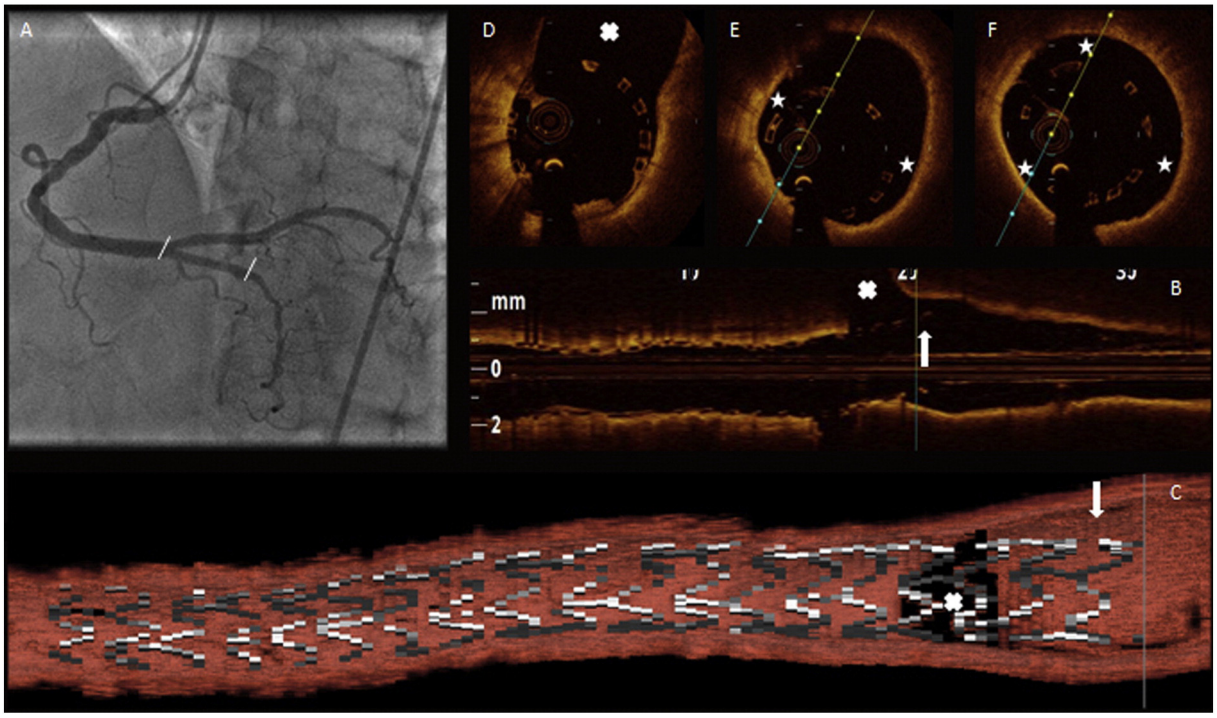

Fig. 2. Scaffold protrusion. Patient was implanted with a 2.5 mm scaffold in PDA. (A) Angiographically optimal result. (B) OCT longitudinal view and 3 D reconstruction (C) showing protrusion of scaffold into distal RCA (arrow). (D–F)Cross sectional images showing scaffold protrusion with malapposition (*). X – origin of posterolateral ventricular branch.

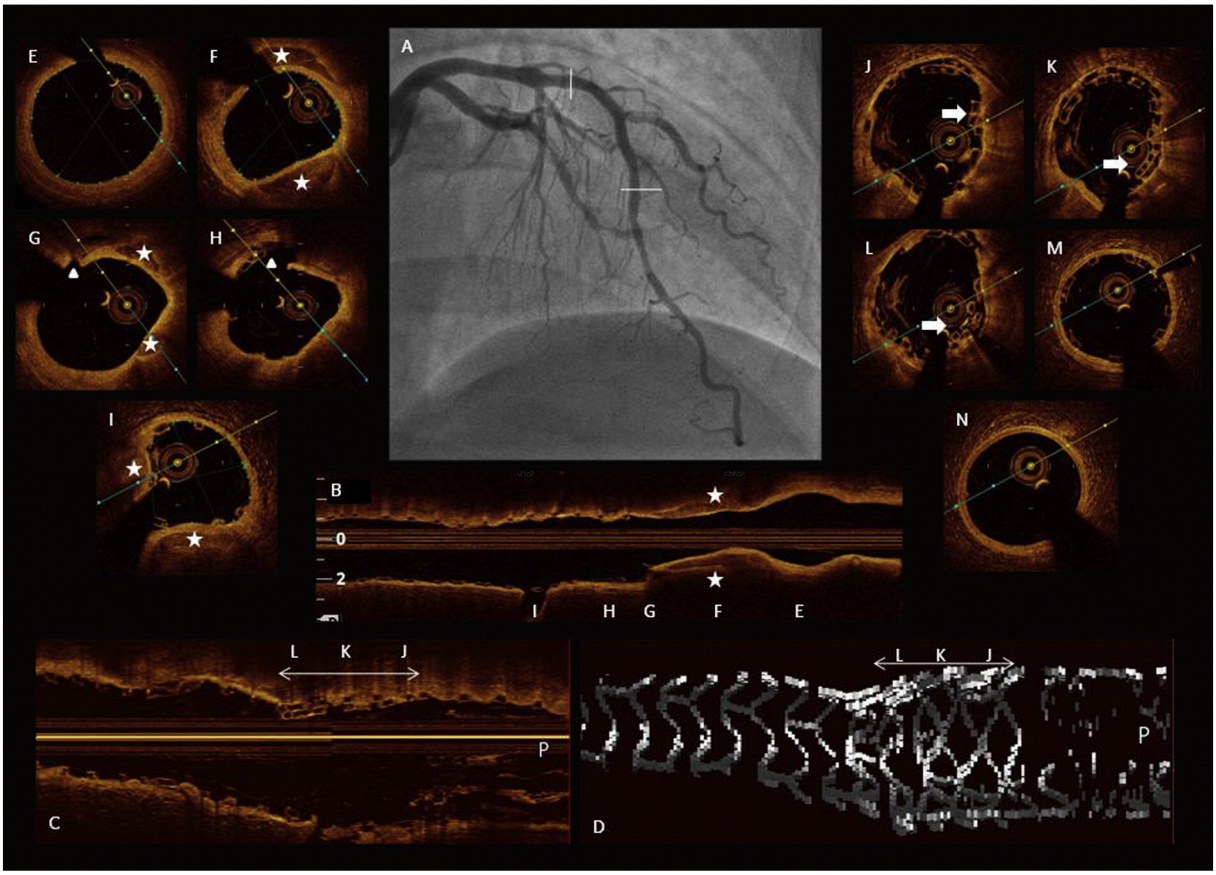

Fig. 3. Excessive overlap and geographic miss. Patient was implanted with 3 and 3.5 mm overlapping scaffolds in mid LAD. (A) Angiographic image showing scaffold boundaries (lines) and proximal geographic miss (balloon dilated segment not covered with scaffold). (B) OCT longitudinal image showing calcific plaques at the proximal edge (*). (C & D) overlap segment (4.9 mm). (E–N) cross sectional OCT images showing calcific plaques (E, G, I,*), minor edge dissection (G&H, triangle), minimum lumen area (I), overlaps segment (J–L, arrow), distal scaffold segment (M) and distal reference(N). M and N are not shown in longitudinal views.

OCT sub-study of ABSORB cohort B trial involving 3 mm scaffolds, the expansion criteria of >5 mm^2 was not met in 56% of the patients. Most of them occurred in the subset of the patients with Dmax of <2.5 mm [15]. The expansion criteria used in the present study was based on three assumptions: (1) the scaffold was appropriately sized to the vessel, (2) there is very limited overexpansion capacity, and (3) only limited sizes of scaffolds are available. 80% of the maximal achievable area to the size of the scaffold was defined as appropriate expansion. With this criterion, 22 scaffolds showed at least one frame of underexpansion. Underexpansion was commonly observed with 3 mm scaffolds and largely resulted from implantation in smaller sized vessels where the scaffolds even failed to meet the expansion criteria for 2.5 mm size in significant number of the frames. The larger scaffolds implanted in smaller vessels were not associated with any significant adverse events in the current study as with the ABSORB cohort B trial [24].

4.2. Scaffold malapposition

With the introduction of intravascular imaging, malapposition is commonly being observed with metal stents. OCT with its superior resolution detects malapposition more often than IVUS [25,26]. Malapposition was noted in 75% of the lesions in the ABSORB cohort B trial OCT sub-study. In this study >5% malapposed struts in a scaffold was defined as one of the criteria of suboptimal scaffold deployment. The mean percentage of malapposed struts was 6.2% and >5% malapposed struts per scaffold was observed more commonly in patients implanted with 3 mm scaffold in vessels with Dmax of >3.3 mm (66.7%) compared to those with Dmax 2.5–3.3 mm (36.7%) and Dmax < 2.5 mm (7.7%) [15]. Based on the underlying mechanism, we divided malapposition into different categories. However, the exact clinical significance of these patterns of malapposition is currently not clear. In major imaging studies, malapposition was not associated with poor outcomes provided the stent was optimally implanted otherwise [27]. In the series by Karanasos et al. [8], there was no difference in the incidence of frame level malapposition between the frames with or without thrombus. Though the malapposition area was higher in frames with thrombus, it did not reach statistical significance. Malapposition related to underlying calcified plaque and side branch were the common types of malapposition in these studies and they may not be associated with poor outcomes in the presence of optimal stent areas. The same prognostic significance may not apply to other subtypes. In case of malapposition related to scaffold undersizing, it may not be possible to expand the scaffold to a large extend because of its limited expansion capacities. The same apply to malapposition related to ectasia and scaffold protrusion. All these may sometimes result in extensive areas of malapposition. Though small malappositions may disappear in the due course of time, malappositions of large magnitude may persist and continue to pose risk of thrombosis until they disappear completely. Secondly, scaffold malapposition resulting from distortion has been reported to be associated with ischemic events at follow up and may require intervention with DES [12]. Though none of our patients met the criteria for >5% of malapposed struts per scaffold, we observed malapposition related to ectasia, protrusion, and distortion. All these patients were kept on newer antiplatelet agents and close

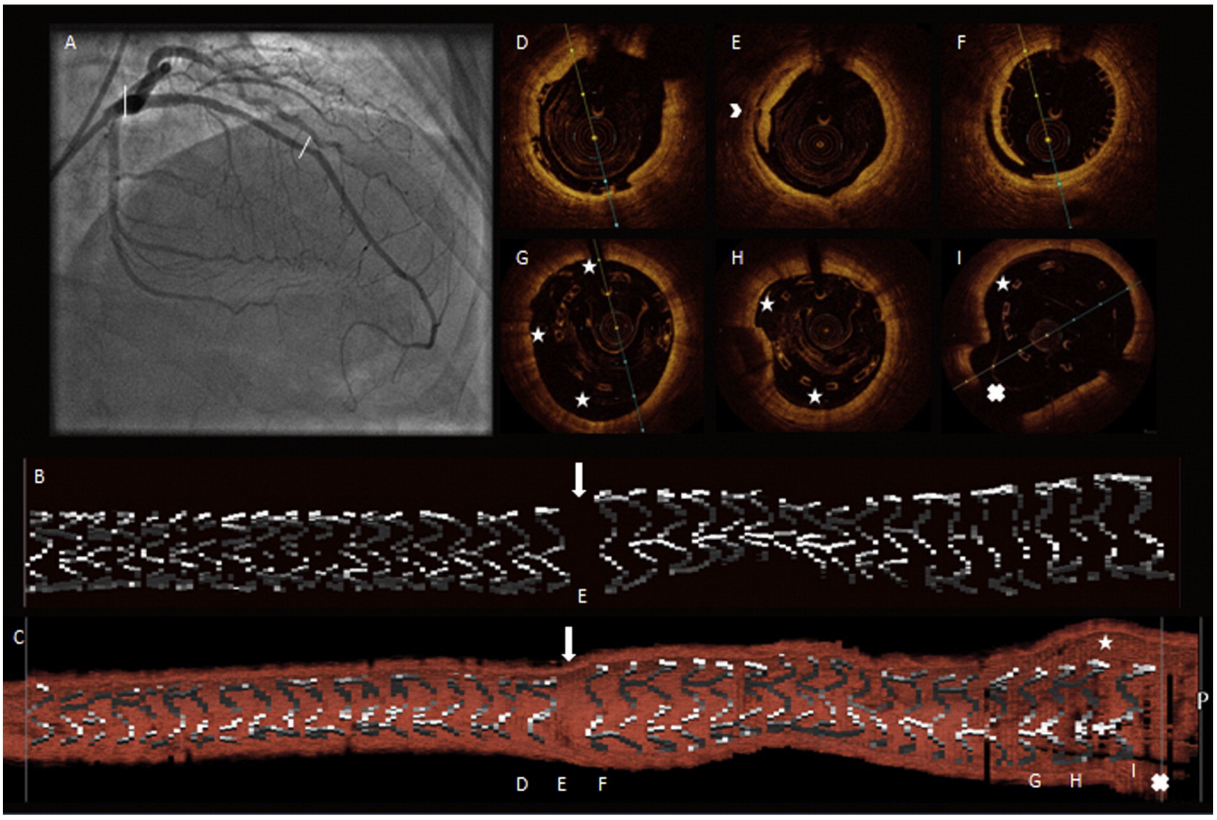

Fig. 4. Scaffold gap. Patient was implanted with 3 mm scaffold in the proximal LAD and additional 2.5 mm scaffold distally for edge dissection. (A) Angiographically optimal final result. (B & C) 3D reconstruction OCT images showing scaffold gap (arrow) and malapposition (*) and overhang of the proximal end of the scaffold (X). (D–I) cross sectional OCT images showing scaffold gap with uncovered dissection (E, arrow head), malapposition in the ectatic segment (G, H,*) and overhang (I). X- origin of LCX.

clinical follow up. Though there were no adverse events in our cohort during the follow up, it remains to be seen whether same continues until the disappearance of the scaffold.

4.3. Scaffold pattern irregularities/fracture

Scaffolds are prone for loss of structural integrity or fracture of the struts when they are subjected to certain deforming forces. In the absorb cohort B study, there were 3 cases of SPI/F and were all related to post dilatation with oversized balloons to correct scaffold under expansion in two cases and major malapposition in the third. The last patient required target lesion revascularization at 33 days for ischemic symptoms [15]. One other case of SPI resulted while crossing into the side branch with OCT catheter [28]. We observed scaffold deformation in a patient who underwent ostial RCA scaffold implantation. Though the expansion capacity of the scaffold was not exceeded during post dilatation, the scaffold developed deformation probably from guide catheter manipulation post balloon dilatation. Currently the exact consequences of scaffold pattern irregularities and its management are not clear. They may result in scaffold failure from flow disturbances triggered by protruding struts. In addition to the risk of SPI/F, BVS may not be an ideal option for aorto-ostial lesions due to its limited radial strength. Moreover poor visibility of the scaffold makes it extremely difficult to identify the scaffold pattern irregularity angiographically and OCT imaging is difficult to obtain in these ostial lesions [29,30].

4.4. Tissue prolapse and edge dissection

Tissue prolapse is noticed commonly in patients with acute coronary syndrome undergoing stent implantation. Though it has been linked to increase in periprocedural CK-MB elevation, it does not influence the long term outcomes provided the residual lumen area remains adequate [18,31,32]. Mattesini et al. [5], observed slightly higher tissue prolapse volume with BVS compared to DES. Though tissue prolapse >10% of the scaffold area was noticed in 7 of our patients, the operators decided not to intervene in any of them. There were no adverse events associated with tissue prolapse in the cohort.

Edge dissections are common findings in OCT imaging following stent implantation. Most of the dissections are angiographically silent and do not compromise flow. These minor dissections are not usually associated with any adverse events and heal on follow up [18]. However, flow limiting dissections or intramural hematoma may result in acute vessel closure and need additional intervention [33]. Mattesini et al. [5], observed 5 edge dissections with OCT following BVS implantation. None of them were angiographically visible and were left alone. In our cohort, there were 3 major dissections and two of them were visible angiographically and one appeared as a hazy lesion and OCT showed intimal dissection with flap protruding into the lumen. Remaining 6 dissections were non-flow limiting and were not associated with any adverse events on follow up.

4.5. Geographic miss

Geographic miss resulting either from failure to cover the injured vessel segment or residual disease at edge has been linked to adverse outcomes in angiographic studies [34]. Similarly, the plaque burden at the stent edges have been shown to be correlated with edge restenosis at follow up in IVUS studies [35]. Though it may not always possible to estimate the plaque burden with OCT, it is possible to measure the lumen area and the presence of disease at the scaffold edges. In the ABSORB Cohort B trial, there were two cases of proximal edge restenosis probably related to geographic miss, the first one related to edge injury from the guiding catheter and the second one from the uncovered predilated segment [11]. In the case series of BVS failure from GHOST

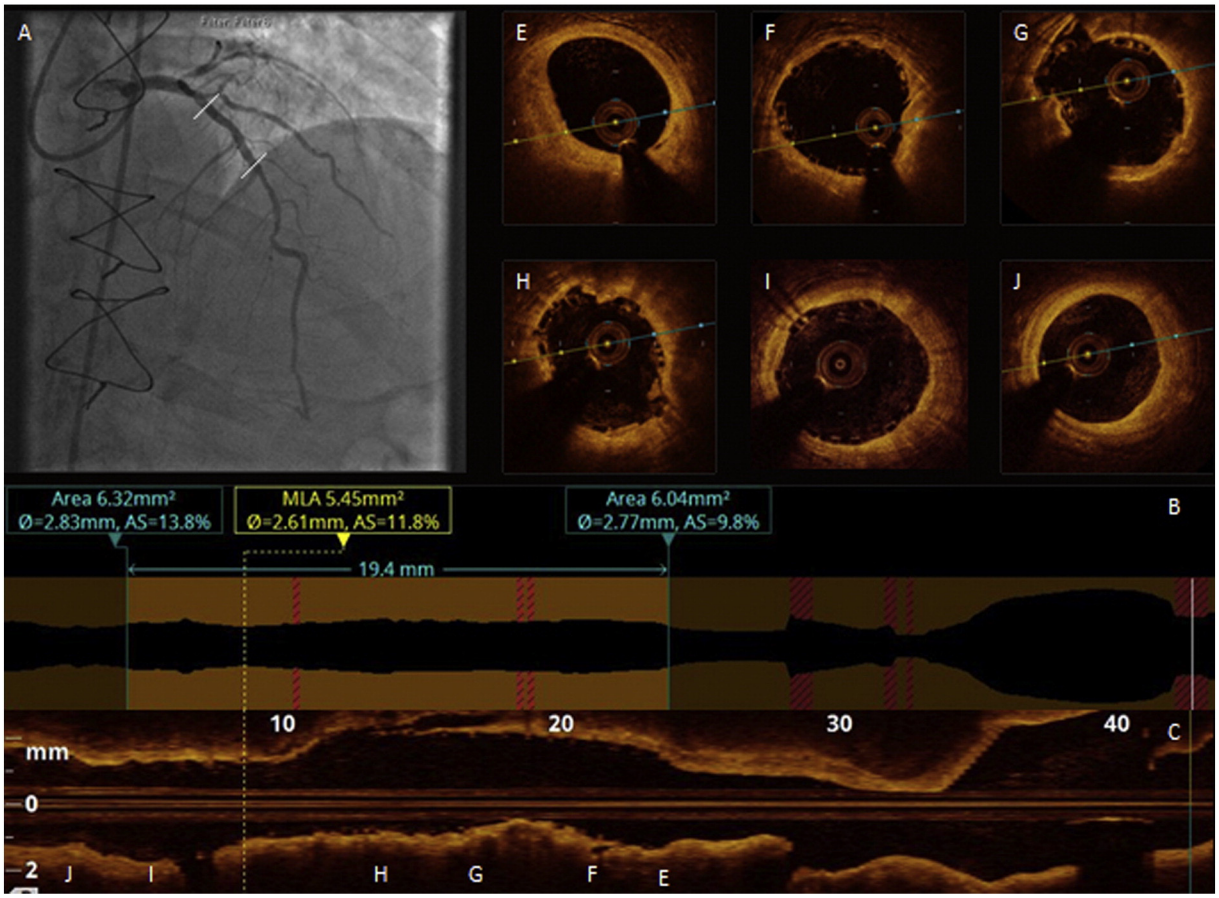

Fig. 5. Longitudinal elongation. Patient was implanted with a 3 mm scaffold in mid LAD calcified lesion after cutting balloon dilatation. (A) Angiographically optimal result. (B & C) OCT lumen profile and longitudinal view showing scaffold longitudinal elongation. (Final scaffold length – 19.4 mm). (E–J) OCT cross sectional images showing well expanded scaffold with no structural irregularity (F–I), and optimal lumen areas at proximal (E, 4.9 mm^2) and distal (J, 5.8 mm^2) reference segments with no edge dissection.

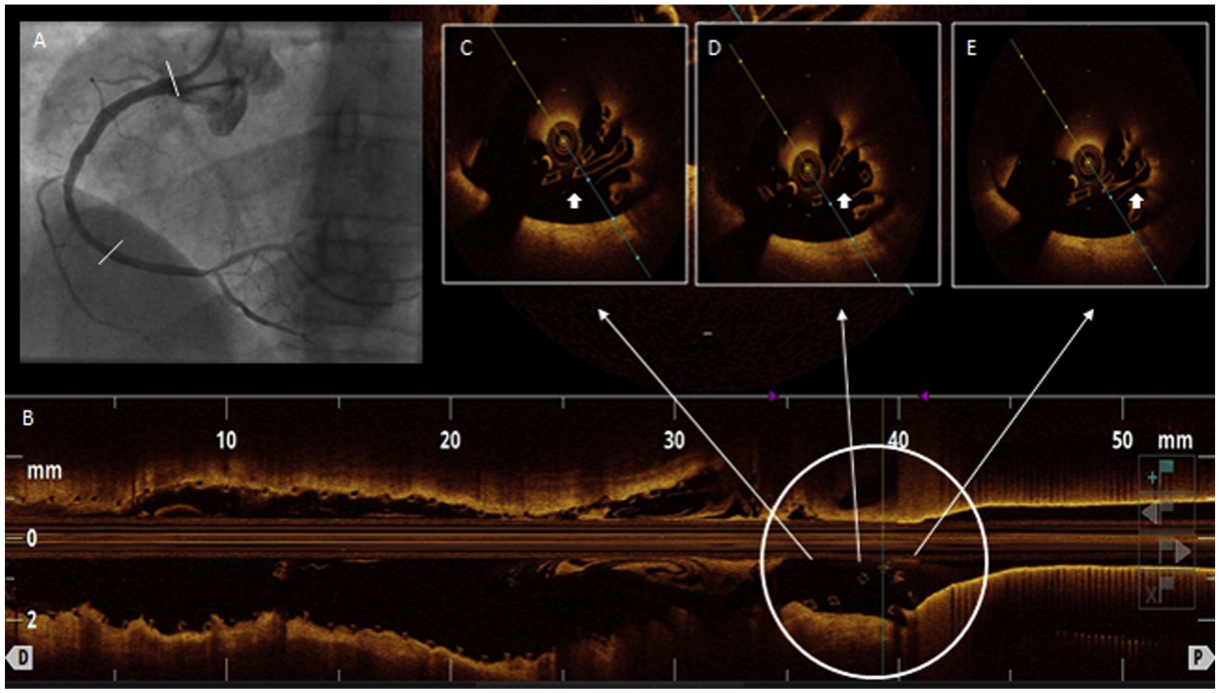

Fig. 6. Scaffold pattern irregularity/fracture. Patient underwent two 3.5 overlapping scaffolds implanted in proximal to mid RCA (lines in A). (A) Angiographically optimal final result. (B) OCT longitudinal view showing deformed scaffold at the ostial RCA (circle). (C–E) OCT cross sectional images showing loss of scaffold structural integrity (Arrows, stacking pattern with malapposition). Blood swirls from incomplete contrast flush obscured part of the scaffold.

registry, there were 6 edge restenosis (Mehran type IB) [14] and were proposed to relate to abnormal edge vascular response or geographic miss [10]. In the series by Karanasos et al. [8], incomplete lesion coverage was observed in three patients with scaffold thrombosis, resulting either from incomplete coverage of the predilated segment or the segment with thrombus in a patient with ST-segment elevation myocardial infarction. Of the 3 cases with geographic miss in our series, one at the proximal edge was left alone as the lumen area was adequate. In other two cases, the scaffold edge landed in a large plaque with small lumen area. Both were left alone without further intervention. There were no events related to geographic miss during follow up.

4.6. Suboptimal scaffold overlap

BVS is available only in limited lengths and hence overlapping becomes necessary for long lesions. Various methods have been proposed to achieve accurate overlapping of scaffolds [36,37]. Though the radiopaque markers help in positioning the second scaffold with minimal overlap, invisibility of the scaffolds makes this process cumbersome. This results in either longer overlap or gap between scaffolds. The exact consequences of these abnormalities are not known. Most of the published data with BVS are with single scaffolds without overlap. One of the case of scaffold thrombosis in Karanasos et al. [8] series resulted from longer scaffold overlap in the absence of underexpansion and malapposition. In the ABSORB EXTEND trial, one of the early scaffold thromboses was related to scaffold overlap with thrombus localized to the overlap region [9]. Further, in the case series from GHOST registry, prominent neointimal hyperplasia was observed at the overlap site in one of the patients and in the gap between the scaffolds in another patient. Overlap sites with double the thickness of scaffold struts may result in flow disturbances that may predispose to scaffold thrombosis [9] or excessive neointimal hyperplasia and instent restenosis. In contrast, gap between the scaffolds may prevent exposure to the drug and resultant restenosis [10]. Six patients (8 overlaps, 7 analyzed) had overlapping stent implantation in our series. The overlap was appropriate only in three of them. This again shows the difficultly experienced in overlapping the scaffolds. Though, all of them doing well during the follow up, they may require close follow up.

4.7. Scaffold elongation

The scaffolds may get elongated when faced with resistance from underlying hard fibrous/fibro-calcific plaques during deployment [13,38]. Ohno et al. [38], described a case of longitudinal elongation of a 3 × 18 mm scaffold implanted at 16 atm. Post implantation, the scaffold measured 20.4 mm in length (14.4% elongation), and when compared to another scaffold without elongation, the struts were thinner (131 ± 7 μ vs 154 ± 2 μ). The same group further assessed longitudinal elongation in a population of 29 patients implanted with 31 scaffolds. 17 (54.8%) of those scaffolds showed longitudinal elongation (mean ± SD: 7.98 ± 4.42%) and none showed compromise in scaffold integrity. They also noticed numerically higher rate of calcified plaques and significantly smaller lumen areas in elongated scaffolds compared to scaffolds that were not elongated [13]. We observed elongation in 38.9% of the scaffolds. Similarly, elongation was not associated with SPI/F. However, in contrast to Attizzani et al. [13], all the length measurements were made at the end of the procedure rather than immediately following scaffold deployment and there was no comparison made between the scaffolds with and without elongation on scaffold areas and plaque characteristics. Longitudinal elongation may result in geographic miss, excessive overlapping (long lesions), excessive overhang (ostial lesions) and difficult side branch access (bifurcation lesions) [38]. However, as in previous study, none of our patients with elongation had adverse events during the follow up. Elongation may be a temporary phenomenon. With its elastic properties the scaffold may revert back to its normal length in the due course of time as shown in one of our patients.

4.8. Scaffold protrusion

Branch ostial scaffold implantation is often associated with protrusion of a length of the scaffold into the main branch. Major scaffold protrusions may impede entry into the other branch for further intervention and in addition, malapposition may alter flow dynamics adversely and makes the scaffold prone for thrombosis. One of the cases of scaffold thrombosis in Karanasos et al. [8] series resulted from LAD scaffold protruding into the left main coronary artery. In contrast to DES, the scaffold may offer some advantages in this situation. As the struts may dissolve in the due course of time, the side branch may be totally unjailed [39]. However, there are two important observations worth considering. Firstly, there is a report showing slow resorption of the protruding struts compared to apposed ones [40]. Secondly, BVS promotes strut coverage with neointima even on the malapposed struts. This results in formation of tissue bridges constituting a neocarina. Though this neocarina may protect against scaffold thrombosis, it may also alter the hemodynamics in the main branch behind the neocarina which in turn may promote neointimal proliferation and restenosis [41]. All our patients with significant scaffold protrusion were put on either prasugrel or ticagrelor in addition to aspirin and there were no events in these patients during the follow up.

5. Limitations

The major limitation of the current study was its retrospective nature and the limited population size. The study was intended to analyze the prevalence of the markers of suboptimal deployment by a highly sensitive imaging modality and relate them to clinical outcomes. Though the markers of suboptimal deployment are common in routine practice, the small clinical event rate with BVS may require a large number of patients to derive a meaningful conclusion. We assessed the patients in this population presenting with events related to the scaffold with repeat intravascular imaging. In addition, it continues to follow up other patients till the proposed disappearance of the scaffolds at 4 years and does a final imaging study. This may shed important insights into the proposed advantage of BVS over the current generation DES in the presence certain forms of suboptimal scaffold deployment such as overhang which otherwise remains a continuous threat for very late scaffold thrombosis with DES. Secondly, the OCT criteria for optimal scaffold deployment are derived from studies of DES. Whether, the same criteria would be applicable to the BVS with its different biomaterial properties is currently largely unknown. Thirdly, preprocedural OCT was not available in most of the patients and the influence of preprocedural OCT on post procedure occurrence of markers of suboptimal scaffold implantation is not known. Here again the intention was to assess the prevalence of parameters of suboptimal deployment with angiogram based scaffold implantation. Fourthly, the scaffold sizing was not based on QCA criteria which resulted in inappropriate sizing of the scaffold in a significant number of the patients. However, this reflects the real world scenario and in the ABSORB cohort B trial, similar practice did not result in adverse outcomes [24]. Finally, in three cases, operators intervened further based on the OCT findings and hence, this would have influenced the outcomes based on angiogram alone.

6. Conclusion

OCT features of suboptimal scaffold deployment are common in real world scenario. Underexpansion is the most common parameter of suboptimal scaffold deployment. These were not associated with adverse outcomes on mid-term follow up. However, current findings need to be confirmed in large subset of patients.

Conflict of interest

The authors report no relationships that could be construed as a conflict of interest.

Acknowledgements

None.

References

[1] J. Iqbal, Y. Onuma, J. Ormiston, A. Abizaid, R. Waksman, P. Serruys, Bioresorbable scaffolds: rationale, current status, challenges, and future, Eur. Heart J. 35 (2014) 765–776, http://dx.doi.org/10.1093/eurheartj/eht542 (Epub 2013 Dec 23).
[2] Y. Onuma, D. Dudek, L. Thuesen, M. Webster, K. Nieman, H.M. Garcia-Garcia, et al., Five-year clinical and functional multislice computed tomography angiographic results after coronary implantation of the fully resorbable polymeric everolimus-eluting scaffold in patients with de novo coronary artery disease: the ABSORB cohort A trial, JACC Cardiovasc. Interv. 6 (2013) 999–1009, http://dx.doi.org/10.1016/j.jcin.2013.05.017.
[3] P.W. Serruys, Y. Onuma, J.A. Ormiston, B. de Bruyne, E. Regar, D. Dudek, et al., Evaluation of the second generation of a bioresorbable everolimus drug-eluting vascular scaffold for treatment of de novo coronary artery stenosis: six-month clinical and imaging outcomes, Circulation 122 (2010) 2301–2312, http://dx.doi.org/10.1161/CIRCULATIONAHA.110.970772 (Epub 2010 Nov 15).
[4] A. Abizaid, J.R. Costa Jr., A.L. Bartorelli, R. Whitbourn, v.G. R.J., B. Chevalier, et al., ABSORB EXTEND investigators. The ABSORB EXTEND study: preliminary report of the twelve-month clinical outcomes in the first 512 patients enrolled, EuroIntervention 10 (2015) 1396–1401, http://dx.doi.org/10.4244/EIJV10I12A243.
[5] A. Mattesini, G.G. Secco, G. Dall'Ara, M. Ghione, J.C. Rama-Merchan, A. Lupi, et al., ABSORB biodegradable stents versus second-generation metal stents: a comparison study of 100 complex lesions treated under OCT guidance, JACC Cardiovasc. Interv. 7 (2014) 741–750, http://dx.doi.org/10.1016/j.jcin.2014.01.165.
[6] P.W. Serruys, B. Chevalier, D. Dudek, A. Cequier, D. Carrié, A. Iniguez, et al., A bioresorbable everolimus-eluting scaffold versus a metallic everolimus-eluting stent for ischaemic heart disease caused by de-novo native coronary artery lesions (ABSORB II): an interim 1-year analysis of clinical and procedural secondary outcomes from a randomised controlled trial, Lancet 385 (2015) 43–54, http://dx.doi.org/10.1016/S0140-6736(14)61455-0 (Epub 2014 Sep 14).
[7] D. Capodanno, T. Gori, H. Nef, A. Latib, J. Mehilli, M. Lesiak, et al., Percutaneous coronary intervention with everolimus-eluting bioresorbable vascular scaffolds in routine clinical practice: early and midterm outcomes from the European multicentre GHOST-EU registry, EuroIntervention 10 (2015) 1144–1153, http://dx.doi.org/10.4244/EIJY14M07_11.
[8] A. Karanasos, N. Van Mieghem, D. Van Nienke, F. Cordula, D. Joost, A. Anouchska, et al., Angiographic and optical coherence tomography insights into bioresorbable scaffold thrombosis: single-center experience, Circ. Cardiovasc. Interv. 8 (5) (2015), http://dx.doi.org/10.1161/CIRCINTERVENTIONS.114.002369 (pii: e002369).
[9] Y. Ishibashi, Y. Onuma, T. Muramatsu, S. Nakatani, J. Iqbal, H.M. Garcia-Garcia, et al., ABSORB EXTEND investigators. Lessons learned from acute and late scaffold failures in the ABSORB EXTEND trial, EuroIntervention 10 (2014) 449–457, http://dx.doi.org/10.4244/EIJV10I4A78.
[10] G. Longo, F. Granata, D. Capodanno, Y. Ohno, C. Tamburino, P. Capranzano, et al., Anatomical features and management of bioresorbable vascular scaffolds failure: A case series from the GHOST registry, Catheter. Cardiovasc. Interv. 85 (2015) 1150–1161, http://dx.doi.org/10.1002/ccd.25819 (Epub 2015 Feb 12).
[11] S. Nakatani, Y. Onuma, Y. Ishibashi, T. Muramatsu, J. Iqbal, Y.J. Zhang, et al., Early (before 6 months), late (6–12 months) and very late (after 12 months) angiographic scaffold restenosis in the ABSORB Cohort B trial, EuroIntervention 10 (2015) 1288–1298, http://dx.doi.org/10.4244/EIJV10I11A218.
[12] Y. Onuma, P.W. Serruys, T. Muramatsu, S. Nakatani, R.J. Van Geuns, B. de Bruyne, et al., Incidence and imaging outcomes of acute scaffold disruption and late structural discontinuity after implantation of the absorb Everolimus-Eluting fully bioresorbable vascular scaffold: optical coherence tomography assessment in the ABSORB cohort B Trial (a clinical evaluation of the bioabsorbable everolimus eluting coronary stent system in the treatment of patients with de novo native coronary artery lesions), JACC Cardiovasc. Interv. 7 (2014) 1400–1411, http://dx.doi.org/10.1016/j.jcin.2014.06.016.
[13] G.F. Attizzani, Y. Ohno, D. Capodanno, B. Francaviglia, C. Grasso, C. Sgroi, et al., New insights on acute expansion and longitudinal elongation of bioresorbable vascular scaffolds in vivo and at bench test: a note of caution on reliance to compliance charts and nominal length, Catheter. Cardiovasc. Interv. 85 (2015) E99–E107, http://dx.doi.org/10.1002/ccd.25645 (Epub 2014 Sep 3).
[14] A. Andalib, A. Almonacid, J.J. Popma, Qualitative and quantitative coronary Angiography, in: E.J. Topol, P.S. Teirstein (Eds.), Text Book of Interventional Cardiology, Elsevier, Philadelphia, PA 2015, pp. 911–931.
[15] J. Gomez-Lara, R. Diletti, S. Brugaletta, Y. Onuma, V. Farooq, L. Thuesen, et al., Angiographic maximal luminal diameter and appropriate deployment of the everolimus-eluting bioresorbable vascular scaffold as assessed by optical coherence tomography: an ABSORB cohort B trial sub-study, EuroIntervention 8 (2012) 214–224, http://dx.doi.org/10.4244/EIJV8I2A35.
[16] H.M. Garcia-Garcia, P.W. Serruys, C.M. Campos, M. Takashi, N. Shimpei, J.Z. Yao, et al., Assessing bioresorbable coronary devices: methods and parameters, JACC Cardiovasc. Imaging 7 (2014) 1130–1148, http://dx.doi.org/10.1016/j.jcmg.2014.06.018 (Epub 2014 Nov 10).
[17] A. Chieffo, A. Latib, C. Caussin, P. Presbitero, S. Galli, A. Menozzi, et al., A prospective, randomized trial of intravascular-ultrasound guided compared to angiography guided stent implantation in complex coronary lesions: the AVIO trial, Am. Heart J. 165 (2013) 65–72, http://dx.doi.org/10.1016/j.ahj.2012.09.017 (Epub 2012 Nov 20).
[18] S.Y. Choi, B. Witzenbichler, A. Maehara, A.J. Lansky, G. Guagliumi, B. Brodie, et al., Intravascular ultrasound findings of early stent thrombosis after primary percutaneous intervention in acute myocardial infarction: a Harmonizing Outcomes with Revascularization and Stents in Acute Myocardial Infarction(HORIZONS-AMI) substudy, Circ. Cardiovasc. Interv. 4 (2011) 239–247, http://dx.doi.org/10.1161/CIRCINTERVENTIONS.110.959791 (Epub 2011 May 17).
[19] A.S. Abizaid, G.S. Mintz, R. Mehran, A. Abizaid, A.J. Lansky, A.D. Pichard, et al., Long-term follow-up after percutaneous transluminal coronary angioplasty was not performed based on intravascular ultrasound findings: importance of lumen dimensions, Circulation 100 (1999) 256–261.
[20] K. Fujii, S.G. Carlier, G.S. Mintz, Y.M. Yang, I. Moussa, G. Weisz, et al., Stent underexpansion and residual reference segment stenosis are related to stent thrombosis after sirolimus-eluting stent implantation: an intravascular ultrasound study, J. Am. Coll. Cardiol. 45 (2005) 995–998.
[21] P. de Jaegere, H. Mudra, H. Figulla, Y. Almagor, S. Doucet, I. Penn, et al., Intravascular ultrasound-guided optimized stent deployment. Immediate and 6 months clinical and angiographic results from the Multicenter Ultrasound Stenting in Coronaries Study (MUSIC Study), Eur. Heart. J. 19 (1998) 1214–1223.
[22] Z.A. Ali, How and when to use OCT to improve procedural outcome, Presented at 21st Annual Fellows Course on 16th May 2015, 2015.
[23] M. Baquet, H. Nef, K. Grujic, A. Latib, D. Capodanno, P. Capranzano, et al., Pattern of restenosis after bioresorbable vascular scaffold implantation: angiographic substudy of the European multicentre GHOST-EU Registry, Euro15A-POS033 (2015).
[24] R. Diletti, V. Farooq, C. Girasis, C. Bourantas, Y. Onuma, J.H. Heo, et al., Clinical and intravascular imaging outcomes at 1 and 2 years after implantation of absorb everolimus eluting bioresorbable vascular scaffolds in small vessels. Late lumen enlargement: does bioresorption matter with small vessel size? Insight from the ABSORB cohort B trial, Heart 99 (2013) 98–105, http://dx.doi.org/10.1136/heartjnl-2012-302598 (Epub 2012 Oct 31).
[25] R.J. Russo, P.D. Silva, P.S. Teirstein, M.J. Attubato, C.J. Davidson, A.C. DeFranco, et al., A randomized controlled trial of angiography versus intravascular ultrasound-directed bare-metal coronary stent placement (the AVID Trial), Circ. Cardiovasc. Interv. 2 (2009) 113–123, http://dx.doi.org/10.1161/CIRCINTERVENTIONS.108.778647 (Epub 2009 Feb 20).
[26] H.G. Bezerra, G.F. Attizzani, V. Sirbu, G. Musumeci, N. Lortkipanidze, Y. Fujino, et al., Optical coherence tomography versus intravascular ultrasound to evaluate coronary artery disease and percutaneous coronary intervention, JACC Cardiovasc. Interv. 6 (2013) 228–236, http://dx.doi.org/10.1016/j.jcin.2012.09.017.
[27] E. Im, B.K. Kim, Y.G. Ko, D.H. Shin, J.S. Kim, D. Choi, et al., Incidences, predictors, and clinical outcomes of acute and late stent malapposition detected by optical coherence tomography after drug-eluting stent implantation, Circ. Cardiovasc. Interv. 7 (2014) 88–96, http://dx.doi.org/10.1161/CIRCINTERVENTIONS.113.000797 (Epub 2014 Jan 14).
[28] K. Sato, V.F. Panoulas, T. Naganuma, T. Miyazaki, A. Latib, A. Colombo, et al., Bioresorbable vascular scaffold strut disruption after crossing with an optical coherence tomography imaging catheter, Int. J. Cardiol. 174 (2014) 116–119, http://dx.doi.org/10.1016/j.ijcard.2014.04.186.
[29] H. Kawamoto, N. Ruparelia, T. Miyazaki, K. Sato, A. Latib, A. Colombo, et al., OCT images of longitudinal deformation following bvs implantation in the right coronary ostium, JACC Cardiovasc. Imaging (Jul 15 2015), http://dx.doi.org/10.1016/j.jcmg.2015.04.013 (pii: S1936-878X(15)00354-X (Epub ahead of print)).
[30] T. Gori, J. Wiebe, D. Capodanno, A. Latib, M. Lesiak, S.A. Pyxaras, et al., Use of Absorb bioresorbable scaffolds for the treatment of coronary ostial lesions - results from the GHOST-EU database, Euro15A-POS035 (2015).
[31] Y.J. Hong, M.H. Jeong, Y.H. Choi, J.A. Song, D.H. Kim, K.H. Lee, et al., Impact of tissue prolapse after stent implantation on short- and long-term clinical outcomes in patients with acute myocardial infarction: an intravascular ultrasound analysis, Int. J. Cardiol. 166 (2013) 646–651, http://dx.doi.org/10.1016/j.ijcard.2011.11.092 (Epub 2011 Dec 15).
[32] T. Sugiyama, S. Kimura, D. Akiyama, K. Hishikari, N. Kawaguchi, T. Kamiishi, et al., Quantitative assessment of tissue prolapse on optical coherence tomography and its relation to underlying plaque morphologies and clinical outcome in patients with elective stent implantation, Int. J. Cardiol. 176 (2014) 182–190, http://dx.doi.org/10.1016/j.ijcard.2014.07.005 (Epub 2014 Jul 11).
[33] M.D. Radu, L. Räber, J. Heo, B.D. Gogas, E. Jørgensen, H. Kelbæk, et al., Natural history of optical coherence tomography-detected non-flow-limiting edge dissections following drug-eluting stent implantation, EuroIntervention 9 (2014) 1085–1094, http://dx.doi.org/10.4244/EIJV9I9A183.
[34] M.A. Costa, D.J. Angiolillo, M. Tannenbaum, M. Driesman, A. Chu, J. Patterson, et al., STLLR investigators, impact of stent deployment procedural factors on long-term effectiveness and safety of sirolimus-eluting stents (final results of the multicenter prospective STLLR trial), Am. J. Cardiol. 101 (2008) 1704–1711, http://dx.doi.org/10.1016/j.amjcard.2008.02.053 (Epub 2008 Apr 9).
[35] S.J. Kang, Y.R. Cho, G.M. Park, J.M. Ahn, W.J. Kim, J.Y. Lee, et al., Intravascular ultrasound predictors for edge restenosis after newer generation drug-eluting stent implantation, Am. J. Cardiol. 111 (2013) 1408–1414, http://dx.doi.org/10.1016/j.amjcard.2013.01.288 (Epub 2013 Feb 20).

[36] V. Farooq, Y. Onuma, M. Radu, T. Okamura, J. Gomez-Lara, S. Brugaletta, et al., Optical coherence tomography (OCT) of overlapping bioresorbable scaffolds: from bench work to clinical application, EuroIntervention 7 (2011) 386–399, http://dx.doi.org/10.4244/EIJV7I3A64.

[37] V. Farooq, P.W. Serruys, J.H. Heo, B.D. Gogas, Y. Onuma, L.E. Perkins, et al., Intracoronary optical coherence tomography and histology of overlapping everolimus-eluting bioresorbable vascular scaffolds in a porcine coronary artery model: the potential implications for clinical practice, JACC Cardiovasc. Interv. 6 (2013) 523–532, http://dx.doi.org/10.1016/j.jcin.2012.12.131.

[38] Y. Ohno, G.F. Attizzani, D. Capodanno, C.I. Tamburino, G. Longo, Y. Fujino, et al., Longitudinal elongation, axial compression, and effects on strut geometry of bioresorbable vascular scaffolds: insights from 2- and 3-dimensional optical coherence tomography imaging, JACC Cardiovasc. Interv. 8 (2015) e35–e37, http://dx.doi.org/10.1016/j.jcin.2014.10.012.

[39] T. Okamura, P.W. Serruys, E. Regar, Cardiovascular flashlight. The fate of bioresorbable struts located at a side branch ostium: serial three-dimensional optical coherence tomography assessment, Eur. Heart. J. 31 (2010) 2179, http://dx.doi.org/10.1093/eurheartj/ehq175 (Epub 2010 May 31).

[40] E. Danson, R. Bhindi, P. Hansen, Follow-up evaluation of unapposed bioresorbable vascular scaffold at a coronary bifurcation using optical coherence tomography, Int. J. Cardiol. 177 (2014) 84–86, http://dx.doi.org/10.1016/j.ijcard.2014.10.002.

[41] A. Karanasos, Y. Li, S. Tu, J.J. Wentzel, J.H. Reiber, R.J. van Geuns, E. Regar, Is it safe to implant bioresorbable scaffolds in ostial side-branch lesions? Impact of 'neo-carina' formation on main-branch flow pattern. Longitudinal clinical observations, Atherosclerosis 238 (2015) 22–25, http://dx.doi.org/10.1016/j.atherosclerosis.2014.11.013 (Epub 2014 Nov 18).